Molecular Basis of Light Harvesting and Photoprotection in CP24 UNIQUE FEATURES OF THE MOST RECENT ANTENNA COMPLEX

Passarini, Francesca; Wientjes, Emilie; Hienerwadel, Rainer; Croce, Roberta

Published in:
The Journal of Biological Chemistry

DOI:
10.1074/jbc.M109.036376

Publication date:
2009

THE JOURNAL OF BIOLOGICAL CHEMISTRY VOL. 284, NO. 43, pp. 29536–29546, October 23, 2009

Molecular Basis of Light Harvesting and Photoprotection in CP24

UNIQUE FEATURES OF THE MOST RECENT ANTENNA COMPLEX[*][S]

Received for publication, June 22, 2009, and in revised form, August 7, 2009 Published, JBC Papers in Press, August 21, 2009, DOI 10.1074/jbc.M109.036376

Francesca Passarini[‡], Emilie Wientjes[‡], Rainer Hienerwadel[§], and Roberta Croce[‡1]

From the [‡]Department of Biophysical Chemistry, Groningen Biomolecular Sciences and Biotechnology Institute, University of Groningen, Nijenborgh 4, 9747 AG Groningen, The Netherlands and the [§]Laboratoire de Genetique et Biophysique des Plantes, Département de Biologie, Faculté de Sciences de Luminy, Université d'Aix-Marseille II, 163 Avenue de Luminy, 13288 Marseille, France

CP24 is a minor antenna complex of Photosystem II, which is specific for land plants. It has been proposed that this complex is involved in the process of excess energy dissipation, which protects plants from photodamage in high light conditions. Here, we have investigated the functional architecture of the complex, integrating mutation analysis with time-resolved spectroscopy. A comprehensive picture is obtained about the nature, the spectroscopic properties, and the role in the quenching in solution of the pigments in the individual binding sites. The lowest energy absorption band in the chlorophyll *a* region corresponds to chlorophylls 611/612, and it is not the site of quenching in CP24. Chlorophylls 613 and 614, which are present in the major light-harvesting complex of Photosystem appear to be absent in CP24. In contrast to all other light-harvesting complexes, CP24 is stable when the L1 carotenoid binding site is empty and upon mutations in the third helix, whereas mutations in the first helix strongly affect the folding/stability of the pigment-protein complex. The absence of lutein in L1 site does not have any effect on the quenching, whereas substitution of violaxanthin in the L2 site with lutein or zeaxanthin results in a complex with enhanced quenched fluorescence. Triplet-minus-singlet measurements indicate that zeaxanthin and lutein in site L2 are located closer to chlorophylls than violaxanthin, thus suggesting that they can act as direct quenchers via a strong interaction with a neighboring chlorophyll. The results provide the molecular basis for the zeaxanthin-dependent quenching in isolated CP24.

Under limiting light conditions, plants need to harvest all of the available light to drive the photosynthetic process. To this aim, they are provided with a large antenna system composed of members of the Lhc[2] (light-harvesting complex) family (1), which coordinate chlorophylls (Chls) and carotenoids and increase the absorption cross-section of the system. Under high light conditions, the amount of photons harvested by the photosynthetic complexes exceeds the need of the chloroplast, and to avoid major damage (2), the excess energy is dissipated as heat in a process called nonphotochemical quenching (NPQ) (3, 4). Although the molecular mechanism of this process has not been fully clarified yet, it is clear that Lhcb proteins are involved (5–8). These complexes have thus a double and opposite role of harvesting light under low light conditions and of dissipating the excess energy in high light. Six Chl-binding proteins compose the antenna system of Photosystem II (PSII) of higher plants. The main complex, LHCII, which is the product of Lhcb1–3 genes (9), is present in trimeric form in the membrane. The trimers are located at the periphery of the PSII supercomplex and are connected to the core (which contains the reaction center, where the charge separation occurs) via three other Lhcb members, the so called minor antenna complexes, the products of the genes Lhcb4 (also called CP29), Lhcb5 (CP26), and Lhcb6 (CP24) (10). These proteins are present as monomers in the membrane (11).

Only the structure of LHCII has been obtained at nearly atomic resolution (12, 13), showing the presence of three transmembrane helices, four carotenoids, and 14 Chl molecules per monomeric subunit. Sequence comparison suggests a very similar folding for the other members of the family (1), although biochemical data indicate that the minor antenna complexes bind a smaller number of pigments (14).

CP24 is with Lhcb3 the most recent member of the Lhc family, and it has evolved after the splitting between land plants and algae (15). It is also smaller than the other antenna complexes, lacking the amphipathic helix at the C-terminal domain and having a shorter luminal loop (see Fig. 1). At present, little information is available about this protein because of difficulties in purifying it in its native state (14, 16, 17). This complex was obtained by *in vitro* reconstitution showing that it coordinates 10 Chl molecules and two xanthophylls (18, 19). The recombinant complex was shown to have properties identical to those of the native one (18).

The analysis of the CP24 knock-out mutant of *Arabidopsis thaliana* has indicated that the absence of this protein strongly

* This work was supported by The Netherlands Organization for Scientific Research Earth and Life Science through a VIDI grant and by the Frans/Nederlandse Academie via a Van Gogh grant.

[S] The on-line version of this article (available at http://www.jbc.org) contains supplemental Figs. S1 and S2.

[1] To whom correspondence should be addressed. Tel.: 31-50-363-4214; Fax: 31-50-363-4800; E-mail: R.Croce@rug.nl.

[2] The abbreviations used are: Lhc, light-harvesting complex; β-DDM, *n*-dodecyl-β-D-maltoside; Chl, chlorophyll; CP24, CP26, CP29, chlorophyll protein of 24, 26, 29 kDa; CP24ko, CP24 knockout mutant; L, lutein; Lhcb, light-harvesting complex of Photosystem II; LHCII, major light-harvesting complex of Photosystem II; NPQ, nonphotochemical quenching; PDB, Protein Data Bank; PSII, Photosystem II; TmS, triplet minus singlet; V, violaxanthin; WT, wild type; Z, zeaxanthin.

influences the packing of PSII in the membrane and thus the efficiency of photosynthesis (20, 21). Moreover, plants lacking CP24 are strongly affected in their photoprotection efficiency. Indeed, among all mutants lacking individual Lhcb subunits, CP24ko and CP26/CP24ko double mutant (which has restored photosynthetic efficiency) are the ones showing the strongest effect on the kinetics of NPQ, suggesting that CP24 is a site of zeaxanthin-dependent quenching (21). Recently, it has been proposed that CP24, together with the other minor antenna complexes, is the site of formation of a zeaxanthin radical cation, and thus it is directly involved in NPQ (22, 23). It was also shown that during NPQ a complex consisting of CP29, CP24, and an LHCII trimer dissociates from the Photosystem II supercomplex (24). It was proposed that this dissociation allows PsbS, one of the major players in NPQ (25), to interact directly with CP29 and CP24, switching them to the dissipative conformation. Interestingly, green algae, which lack CP24 (26), have evolved different mechanisms of NPQ (27–29), thus suggesting a correlation between the presence of CP24 (and Lhcb3) and the development of NPQ in land plants.

In this work we have analyzed in detail the properties of the individual chromophores associated with CP24 with particular attention to their role in light harvesting and photoprotection. The data indicate that CP24 differs from the other members of the Lhc family, supporting the hypothesis of a different role for this subunit.

EXPERIMENTAL PROCEDURES

DNA Cloning, Mutagenesis, Recombinant Protein Overexpression, and Pigment-Protein Complex Reconstitution—Lhcb6 (AT1G15820) mature sequence from *A. thaliana* was amplified from cDNA by PCR and cloned in a modified pET-28a (+) carrying a minimum polylinker. Mutant sequences were obtained by site-directed mutagenesis of the codons for Chl-coordinating residues to apolar residues with similar steric hindrance: E188V for the Chl 610 binding site, H191F for Chl 612, E205V for Chl 613, E62V for Chl 602, H65F for Chl 603, Q109L for Chl 606, and E117V for Chl 609. In the case of Chl 610 and 602, whose ligands form ion pairs with two arginines, also the double mutants were obtained (E188V/R67L and E62V/R193L, respectively); because the second mutation reduced the stability of the complex, the analysis has been done on the single mutants. Wild type (WT) and mutant apoproteins were overexpressed in Rosetta2(DH3) strain of *Escherichia coli* and purified as inclusion bodies. Reconstitution of pigment-protein complexes was performed as described in reference 30 using a mix of purified pigments with a Chl *a/b* ratio of 2.9 and Chl/carotenoid ratio of 2.7; in the case of the WT and Chl-binding mutants, a total carotenoid extract from spinach thylakoids was used, whereas in the case of the carotenoid mutants only lutein (CP24-L) or a mix of lutein and zeaxanthin in a ratio 1:1 (CP24-LZ) were used. The purification of the refolded complex from the unfolded protein and the excess of pigments was performed as described previously (30) in three steps at 4 °C: (i) sucrose gradient ultracentrifugation (20 h at 41,000 rpm in a SW41 rotor, 288,000 × *g*); (ii) anionic exchange chromatography; and (iii) a second sucrose gradient, which also allowed us to check the monomeric aggregation state of the refolded protein. After the first gradient, unspecifically bound pigments and remaining unfolded protein were almost completely eliminated by anionic exchange chromatography; the column (packed with EMD-DEAE 650 (S) Fractogel) was equilibrated with 50 mM Tris, pH 7.6, 0.025% β-DDM, and the protein complex was eluted with a linear gradient of 500 mM NaCl, 50 mM Tris, pH 7.6, 0.025% β-DDM. The run was followed by measuring the absorption at 280 and 675 nm and the conductivity (supplemental Fig. S1 for more details).

Steady-state Spectroscopy and Pigment Analysis—Room temperature and 77 K absorption spectra were recorded using a Cary4000 (Varian, Inc.) spectrophotometer at a Chl concentration of about 6 μg/ml in 10 mM HEPES, pH 7.5, 0.5 M sucrose, and 0.03–0.06% β-DDM (70% glycerol for the 77 K measurements). Fluorescence emission spectra were measured using a Fluorolog (Jobin Yvon) spectrofluorometer and corrected for the instrument response. Samples were diluted at a Chl concentration of 0.1 μg/ml in 10 mM HEPES, pH 7.5, and 0.02% β-DDM, the bandwidths were 5 nm in excitation and 2.5 nm in emission. The CD spectra were recorded on a AVIV 62ADS spectropolarimeter at 10 °C; the samples were in the same solution and concentration as described for the absorption.

The pigment complement of the complexes was analyzed by fitting the acetone extract spectrum with the spectra of the individual pigments (31) and by high pressure liquid chromatography analysis (32).

Time-resolved Spectroscopy—Light-induced absorbance changes were recorded at room temperature with a home-built high sensitivity laser-based spectrophotometer as described in reference 33. Samples were diluted to a Chl concentration of about 2 μg/ml in 10 mM HEPES, pH 7.5, and 0.03% β-DDM; anaerobic conditions were obtained incubating the sample with 0.02 mg/ml glucose oxidase, 0.04 mg/ml catalase, and 0.02 mg/m glucose for 15 min. Samples were excited at 640 nm. For a given wavelength, the kinetics of the absorbance change were recorded with variable delay times between the actinic and the detection light pulse ranging from 5 ns to 5 ms. The delay time was obtained by setting the electronic trigger for each laser light pulse, and it was determined with fast silicon detectors (Thorlabs-Det210). For each kinetic trace a set of measurements with 39 increasing delay times was performed. The time between excitations was 300 ms. The kinetics were measured five to seven times and averaged. The GraphPad PRISM program (Graph-Pad Software) was used for globally analyzing the decay kinetics between 200 ns and 5 ms over the 420–570-nm wavelength range. The rising of the signals was analyzed by fitting the data from 7.5 to 200 ns with detecting light pulses spaced every 12.5 ns in the time range from 7.5 to 100 ns. The data were fitted satisfactorily by a combination of a time-resolved (>15 ns) and a time-unresolved (<10 ns) rising component. For each wavelength, the millisecond Chl triplet contribution, determined by the decay kinetic, was taken into account as a constant amplitude for the analysis. To calculate the Chl to carotenoid transfer efficiency, the area of the carotenoid peak (maximum around 510 nm) and of the Chl negative peak (Chl singlet at 430 nm) was used. For the ratio of the extinction coefficients, a carotenoid/Chl *a* value of 1.93 was used. This value was calculated from the areas of the singlet spectra of Chl and carotenoid

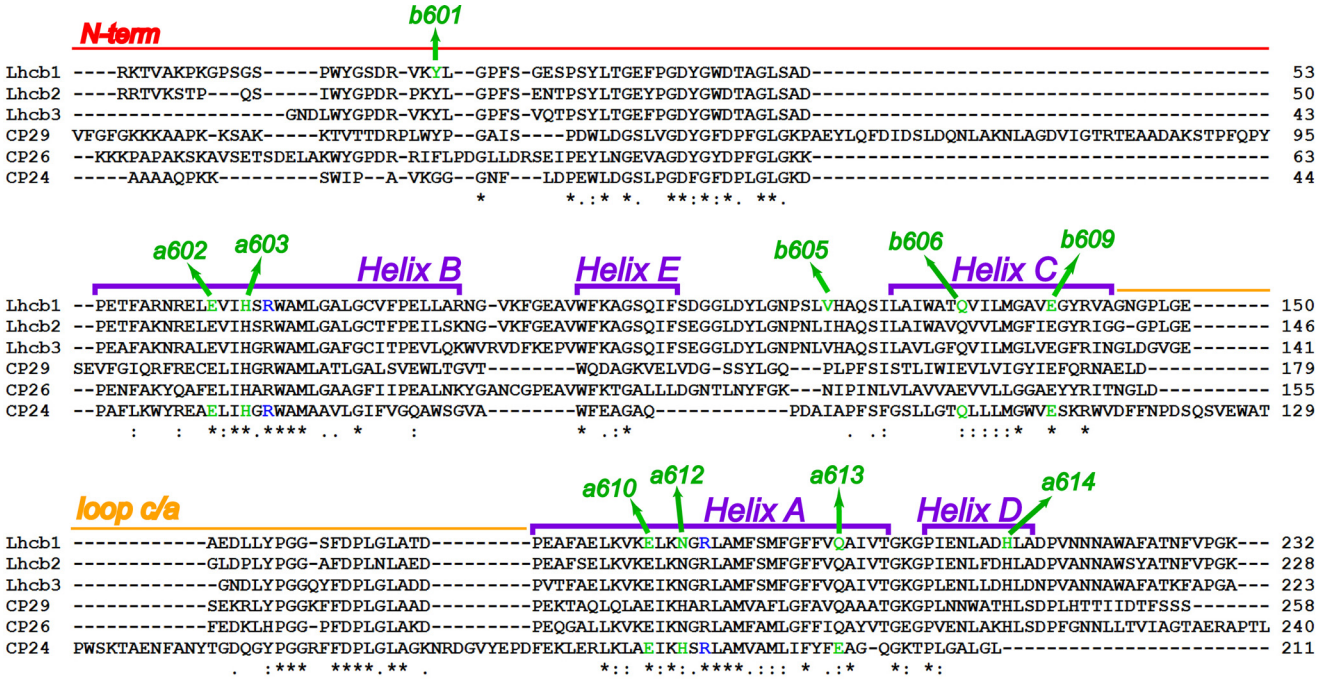

FIGURE 1. **Sequence alignment of predicted Lhcb proteins of *Arabidopsis*.** In the figure, conserved features are highlighted: *red*, the N terminus (*N-term*); *violet*, transmembrane helices; *green*, Chl binding sites (nomenclature from reference 12); *blue*, Arg residues involved in ion pairs between helices B and A; and *yellow*, the stromal loop.

(normalized to their extinction coefficients in ethanol) in the 420–450-nm and 465–540-nm ranges, respectively.

Time-correlated single photon counting was performed with a home-built setup, as described previously (34). In brief, the samples were diluted to an A_{475} of 0.1 cm^{-1} and stirred in a 3.5-ml cuvette with a path length of 1 cm at 10 °C. The excitation was at magic angle with 475-nm pulses at a repetition rate of 3.8 MHz. Pulse energies of sub-pJ were used with a pulse duration of 0.2 ps and a spot diameter of 1 mm. The instrument response function (~60-ps full width at half-maximum) was obtained with pinacyanol iodide in methanol, with a 6-ps fluorescence lifetime (35). Detection was through a 530-nm long pass and a 679-nm interference filter (Schott, Mainz, Germany). Photons were detected by a microchannel plate photomultiplier, and arrival times were stored in 4096 channels of a multichannel analyzer; the channel spacing was 2 ps. Data analysis was performed using home-built software (36). The fit quality was evaluated from the χ^2 and from plots of the weighted residuals and the autocorrelation thereof.

Structural Model of CP24—The model of CP24 was obtained using SWISS MODEL workspace (37) in Alignment model (using the alignment in Fig. 1) with the structure of LHCII (Protein Data Bank (PDB) code 1rwt) as template. The positions of Chls and carotenoids are the same as in LHCII and have been obtained upon aligning the apoprotein model structures of CP24 and LHCII (PDB code 1rwt) in PyMOL.

RESULTS

Sequence alignment of CP24 with the other Lhcb proteins of *Arabidopsis* (Fig. 1) shows that this protein retains most of the Chl-binding residues present in LHCII with the exception of the ligand for Chl 614 (nomenclature of LHCII from ref 12), which is located in the amphipathic helix D, which is absent in CP24. Moreover, the putative ligand for Chl 613 is a Glu and not a Gln as in all other Lhc complexes. CP24 has a His in the position of the ligand for Chl 612, like CP29, but differently from the other complexes where this residue is an Asn. The putative ligand for Chl 606 is a Gln as in Lhcb1–3, whereas this residue is a Glu in the other minor antenna complexes, where it is still able to coordinate Chl (38–40).

Mutation Analysis: Pigment Content, Absorption, Fluorescence, and Circular Dichroism

All putative Chl ligands were mutated into apolar residues, which cannot coordinate the central Mg of the Chl. The proteins were reconstituted with pigments (41), and the refolded complexes were purified from the excess of pigments and the unfolded protein, which does not bind pigments (apoprotein). This was done on the basis of a different migration in sucrose gradient of the holo- and apoproteins and also of their different interactions with the anionic exchange column, probably due to different exposure of the charges, which led to a longer retention time for the apoprotein (see supplemental Fig. S1). All reconstituted complexes were in their monomeric state as assessed by their mobility in sucrose gradient. Moreover, all reconstituted mutants were eluted from the anionic column at the same ionic concentration observed for the WT, thus indicating a very similar folding (see supplemental data for details). In the following, the mutants are named after the Chl the putative ligand of which has been substituted (see *Experimental Procedures* for the list of mutations).

CP24-WT—It is worth nothing that the reconstituted CP24-WT is essentially identical to the native complex extracted from the membranes as was demonstrated previously (see 18 for details). In addition, the recombinant complex can be obtained in far higher amount than the native one and com-

TABLE 1

Pigment composition

The values are normalized to the proposed total number of Chls reported in the last column. The maximal standard deviation is 0.1. V, violaxanthin; L, lutein; Z, zeaxanthin; Tot Cars, total carotenoids; Tot Chls, total chlorophylls.

Sample	Chl *a*/*b*	Chl/Car	V	L	Z	Chl *a*	Chl *b*	V/L	Tot Cars	Tot Chls
CP24-WT	1.08	5.0	1.0	1.0		5.0	5.0	1.0	2.0	10
CP24-L	1.06	5.2		1.9		5.1	4.9		1.9	10
CP24-LZ	1.05	5.6		1.0	0.8	5.1	4.9		1.8	10
Chl 610-mutant	1.06	6.5	0.9	0.3		4.1	3.9	3.0	1.2	8
Chl 612-mutant	0.94	5.9	1.0	0.4		4.3	4.7	2.5	1.4	9
Chl 613-mutant	1.02	5.0	1.0	1.0		5.1	4.9	1.0	2.0	10
Chl 602-mutant	Unstable									
Chl 603-mutant	3.85	5.5	0.4	0.5		4.0	1.0	0.8	0.9	5
Chl 606-mutant	2.04	4.3	0.6	1.0		4.7	2.3	0.6	1.6	7
Chl 609-mutant	1.68	4.2	0.6	1.0		4.4	2.6	0.6	1.6	7

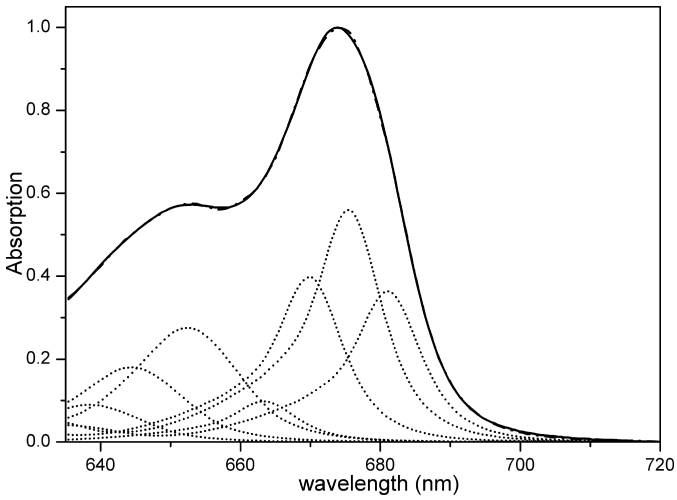

FIGURE 2. **Description of the absorption spectrum of CP24 in terms of individual chlorophylls.** The spectrum can be described satisfactorily using 3 Chl *b* and 4 Chl *a* forms, with maxima, respectively, at 638.5 (with amplitude corresponding to 0.8 Chls), 645.5 (1.8), and 653.5 nm (2.0) for the Chls *b* and at 663 (0.4), 670 (1.6), 675.5 (2.1), and 681 nm (1.4) for Chls *a*.

pletely free from contaminations, thus representing an excellent system for the study of the functional architecture of this complex. The Chl *a*/*b* ratio of CP24-WT (Table 1) is the lowest of all members of the Lhc family (see Table 1 in reference 42, where Lhcb complexes were reconstituted in the same conditions). Assuming a stoichiometry of 10 Chls/polypeptide (18), this complex coordinates 5 Chls *a* and 5 Chls *b*. CP24-WT also binds two xanthophyll molecules, one violaxanthin, and one lutein. The 77 K absorption spectrum of the complex is characterized by the presence of several components as can be assessed by second derivative analysis: two main Chl *a* forms peak at 670.0 and 676.4 nm and four Chls *b* forms around 637 nm, 644 nm, 650 nm, and 655 nm (data not shown). Using these values as starting points, the room temperature absorption spectrum of CP24 was fitted with the spectra of Chl *a* and Chl *b* in protein environment (43) (Fig. 2).

To determine the occupancy of the various binding sites, to assign the absorption forms to individual pigments, and to detect possible pigment-pigment interactions, the refolded mutated complexes were studied by absorption, fluorescence, and circular dichroism (CD) spectroscopy as well as pigment analysis (Table 1). In the following, the biochemical and spectroscopic properties of each mutant are compared directly with those of the WT.

Chl 610- and Chl 612-Mutants—The ratio violaxanthin/lutein of both mutants (Table 1) is very high compared with the WT, indicating the selective loss of lutein. Normalizing the pigments to the violaxanthin content, it can be calculated that Chl 610-mutant loses 1 Chl *a*, 1 Chl *b*, and 0.7 lutein and Chl 612-mutant 1 Chl (mainly Chl *a*), and 0.6 lutein. These numbers should be considered as lower limits because a small loss of violaxanthin cannot be excluded. The severe loss of lutein indicates that in the WT the L1 carotenoid binding site (Lut620 in reference 12), which is in close proximity to Chls 610 and 612 (see Fig. 8), is occupied by lutein, whereas violaxanthin is accommodated in site L2 (Lut621 in 12). It should be underlined that the mutations have a local effect on the structure of the complexes as indicated by the analysis of the CD spectra (Fig. 3*C*). The CD spectrum in the visible region has an excitonic origin, and it is thus extremely sensitive to even small changes in the organization of the pigments. The CD spectra of both mutants are identical to that of the WT but for a specific feature in the red region of the spectrum, which is due to the direct effect of the mutations (see below).

The absorption spectra of the mutants at 77 K are presented in Fig. 3*A* together with the spectrum of the WT. A clear loss of signal at 495 nm is visible in both mutants due to the absence of absorption of lutein in L1. The characteristics of absorption and CD spectra of Chl 612-mutant (Fig. 3*C*) are identical to what was reported previously (44), confirming the presence of a strong interaction between Chls 611 and 612, which is responsible for the 670/680 nm bands.

The absorption difference spectrum of WT minus Chl 610-mutant (Fig. 3*B*) shows a number of bands in the Chl *a* and Chl *b* absorption region, suggesting that the mutation affects the absorption of several Chls. Likely, the partial absence of lutein in L1 influences Chl 612, leading to a change in its interaction with Chl 611. This is supported by the CD spectrum (Fig. 3*C*), where a loss of signal at 682 and 670 nm is visible, but it is less intense than in Chl 612-mutant, indicating that only part of the complexes has lost the interaction. A rough estimate of the absorption of the two Chls lost in the Chl 610-mutant can thus be obtained by subtracting the difference spectrum of Chl 612-mutant from that of Chl 610-mutant, after normalization in the red (not shown). Two bands appear at 670 and 650 nm, which should represent the absorption of Chl 610 and (most likely) that of Chl 608, which in LHCII is located in close proximity to Chl 610 (12). Analysis of the fluorescence emission spectra supports this assignment. The emission of Chl 612-mutant is 2 nm

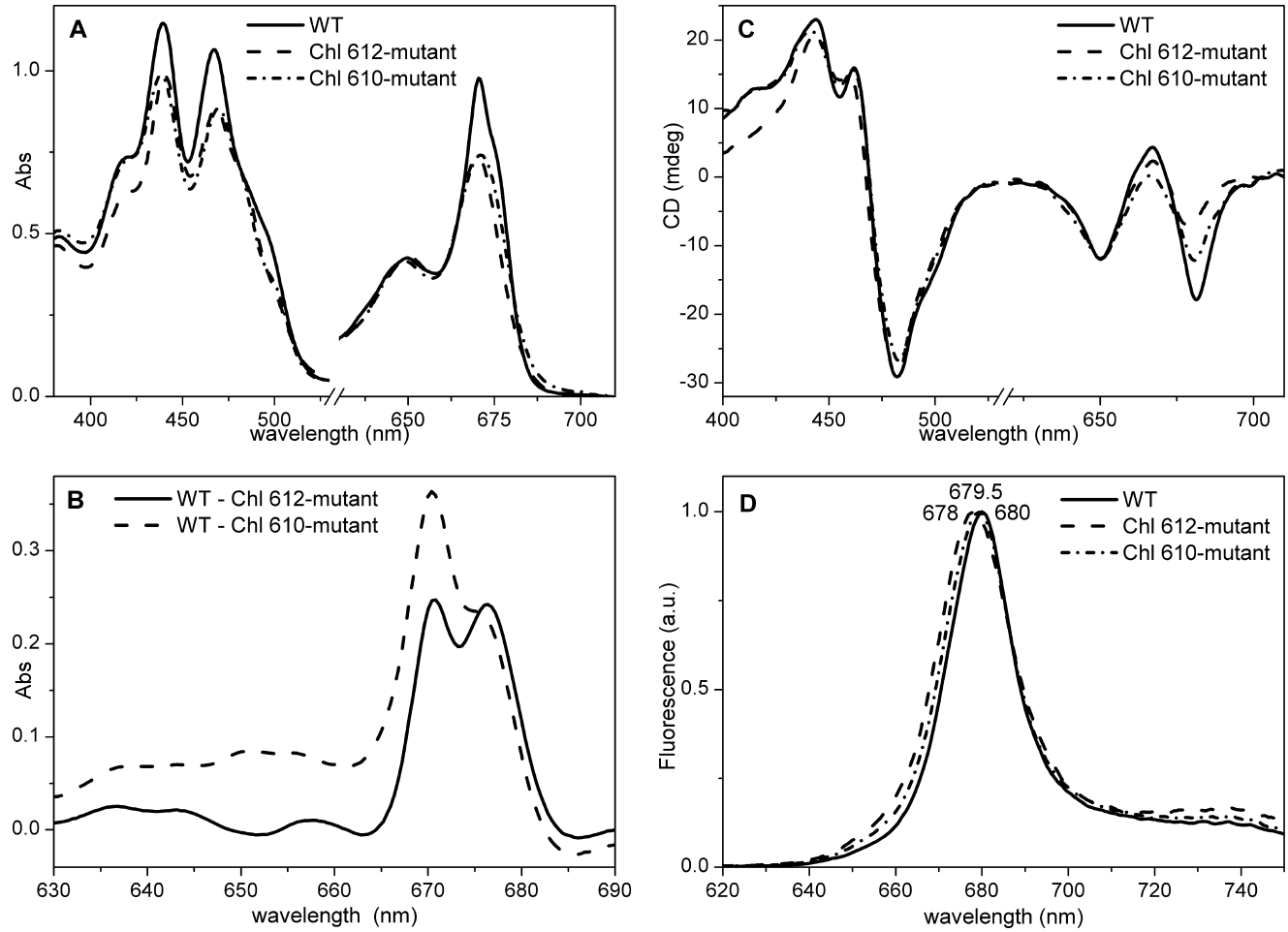

FIGURE 3. **Spectroscopic characterization of Chl 610- and Chl 612-mutants.** *A*, *C*, and *D*, the spectrum of the WT is also shown. *A*, absorption (*Abs*) spectra at 77 K normalized to the Chl content. *B*, difference absorption spectra WT minus mutant. *C*, CD spectra and *D*, fluorescence emission spectra upon excitation at 500 nm.

blue-shifted compared with that of the WT, indicating that Chls 611/612 represent the lowest energy state of the complex. Instead, the emission of Chl 610-mutant is only 0.5 nm blue-shifted (Fig. 3*D*) in agreement with a partial loss of the 612/611 interaction and with the fact that Chl 610 does not contribute to the low energy state in this complex.

Chl 613-Mutant—The mutant at the putative ligand of Chl 613 has the same pigment composition as the WT (Table 1). The shape of the absorption spectrum of the mutant is also identical to that of the WT as well as the CD spectrum (data not shown). This indicates that the mutation does not induce loss of Chl and does not influence the structure of the complex, leading to the conclusion that Glu^{205} is not a Chl ligand in CP24 and suggesting that Chl 613 is not present in this complex.

Chl 606- and 609-Mutants—Both of these mutations strongly affect the folding and/or stability of the protein as indicated by the fact that only a small amount of refolded complexes could be obtained. Both mutated complexes show a higher Chl *a*/*b* ratio compared with the WT, indicating the preferential loss of Chl *b*. The violaxanthin/lutein ratio is decreased, suggesting the specific loss of violaxanthin, in agreement with its location in the L2 site (Table 1). Normalization to the lutein content gives for both mutants a stoichiometry of 7 Chls/polypeptide, which should be considered the upper value. Of the three Chls lost, 2.2–2.5 are Chls *b* and 0.5–0.8 Chls *a*. The room temperature absorption spectra show strong reduction in both Chl *a* and Chl *b* regions in the mutants (Fig. 4*A*). The difference spectrum also shows a contribution at 499 nm, which can be assigned to violaxanthin in the L2 site.

In LHCII, the domain in between the helices B and C is characterized by the presence of an extended network of H-bonds which stabilize the binding of Chls *b* in several sites (12). Thus, the mutations do not only influence the binding of one Chl, but also the binding of neighboring Chls coordinated by water molecules that participate to the H-bonds network (39). The loss of several chromophores in the mutants suggests that also in CP24 the Chls located in this region are strongly interconnected. Moreover, the absorption difference spectra (Fig. 4*B*) strongly resemble those of the same mutants of LHCII (see Fig. 9 in ref. 39) and the ratio of the Chl *a*/Chl *b* bands is higher than expected based on the pigment stoichiometry. This is a signature of Chl *b*-Chl *a* excitonic interactions, in which dipole strength redistribution is favoring the Chl *a* absorption, as is the case in LHCII (45). The data strongly suggest that in CP24 the domain between helices B and C has an organization that is very similar to that of LHCII.

Chl 602- and 603-Mutants—Upon mutation of the putative ligand of Chl 602, no refolded protein could be obtained. This

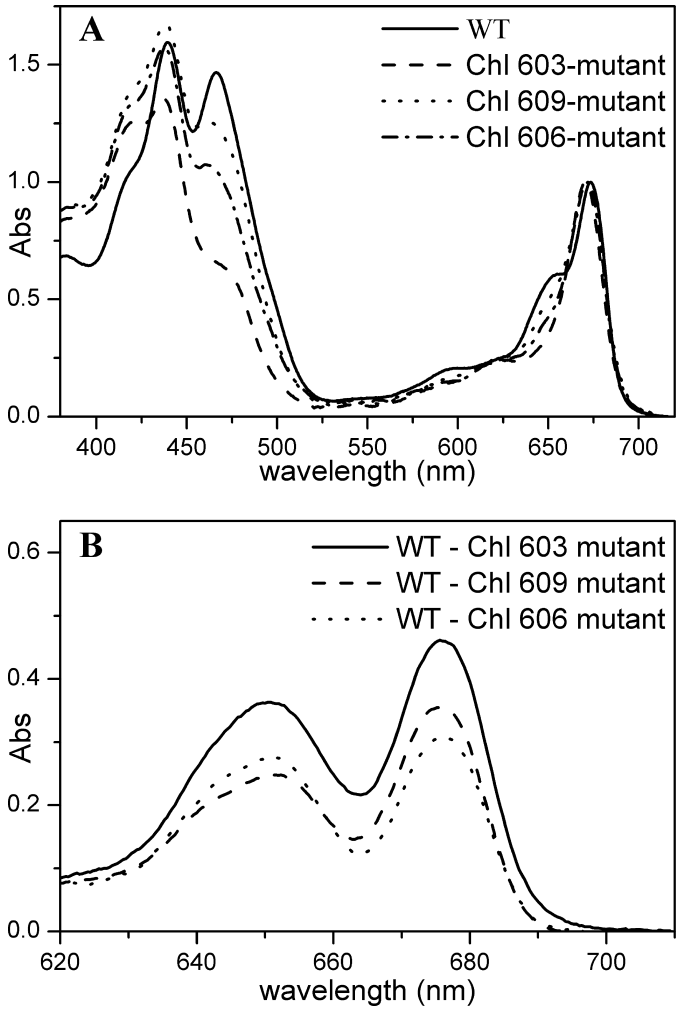

FIGURE 4. **Absorption spectra of CP24-WT and Chl 603-, 606-, and 609-mutants.** *A*, absorption (*Abs*) spectra at room temperature normalized to the maximum in the Q_y region. *B*, difference absorption spectra WT minus mutants upon normalization to the Chl content.

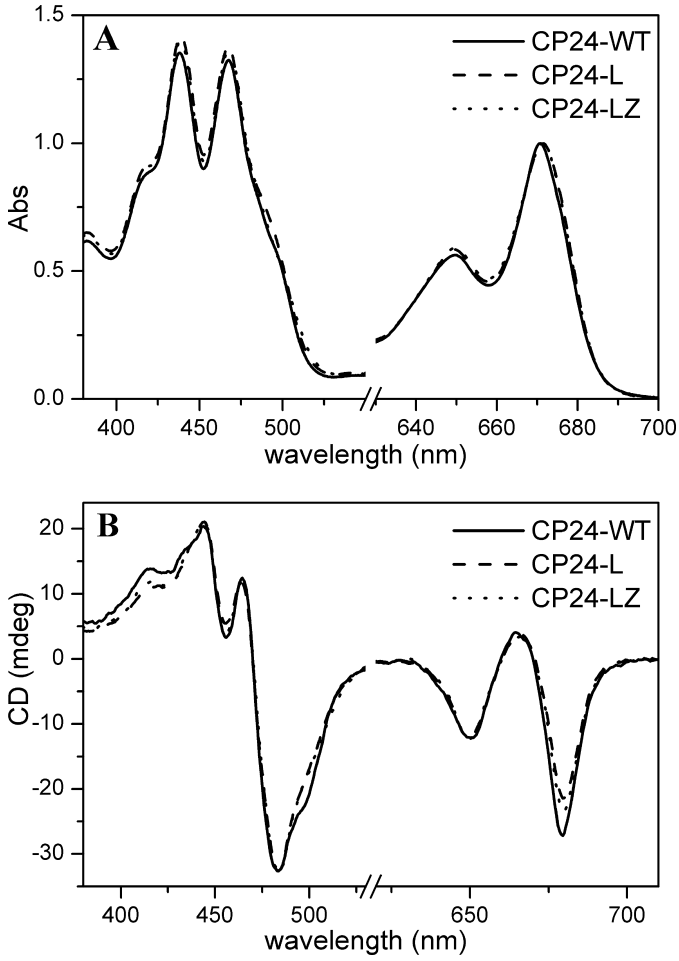

FIGURE 5. **Spectroscopic properties of CP24 with different carotenoid composition.** *Solid lines*, CP24-WT; *dashed lines*, CP24-L; *dotted lines*, CP24-LZ. *A*, absorption (*Abs*) spectra at 77 K. *B*, CD spectra.

indicates that Glu^{62} is essential for the stabilization of the complex, differently from the other related antenna complexes (38–40). Mutation of the ligand of Chl 603 also results in a strongly destabilized complex, as could be assessed by the low reconstitution yield. The Chl *a*/*b* ratio of the mutant is very high, suggesting the loss of 5 Chl molecules, of which 4 are Chl *b* (Table 1). This indicates that the mutation had an influence on a large part of the complex. Indeed, looking at the structure of LHCII, it is observed that the His coordinating Chl 603 is also involved in H-bonding with Chl *b* 609, which takes part in the network of H-bonds connecting several Chls in the helices B and C domain. Apparently, the absence of the His leads to a destabilization of the entire H-bond network and to the loss of most of the Chls involved. In agreement with the pigment analysis, the room temperature absorption spectrum shows a strong reduction of the 650 nm Chl *b* band and a loss of intensity in the Chl *a* region around 676 nm (Fig. 4).

CP24 with Different Carotenoid Composition—Comparison of the pigment content of CP24 with that of the other Lhcb complexes reveals that CP24 coordinates the highest amount of violaxanthin/monomer, namely 1 molecule/complex. De-epoxidation experiments *in vitro* (19) and *in vivo* (17, 46) have indicated that the violaxanthin associated with CP24 is de-epoxidized to zeaxanthin, thus suggesting a role for CP24 in the zeaxanthin-dependent quenching.

To obtain molecular details about the role of each xanthophyll associated with CP24, the complex was reconstituted with a mixture of lutein/zeaxanthin or only lutein. In both cases, a stable complex was obtained. Pigment analysis shows that CP24-L coordinates 2 luteins/polypeptide, and CP24-LZ one lutein and one zeaxanthin (Table 1), suggesting that zeaxanthin has substituted for violaxanthin in the L2 site.

The 77 K absorption spectra of CP24-LZ, CP24-L, and CP24-WT (Fig. 5*A*) are practically identical in the blue region, demonstrating that the spectra of zeaxanthin, lutein, and violaxanthin in the L2 site of CP24 are very similar. This is remarkable considering that the difference in wavelength between the absorption maxima in organic solvent is 8 nm for lutein and zeaxanthin and 12 nm for violaxanthin and zeaxanthin (47). In the Q_y region, CP24-L and CP24-LZ have identical spectra, whereas the spectrum of CP24-WT is blue-shifted, suggesting a change in the environment of some of the Chls (48). This hypothesis is supported by the CD spectra (Fig. 5*B*), which show differences in the Chl *a* Q_y band and in the carotenoid absorp-

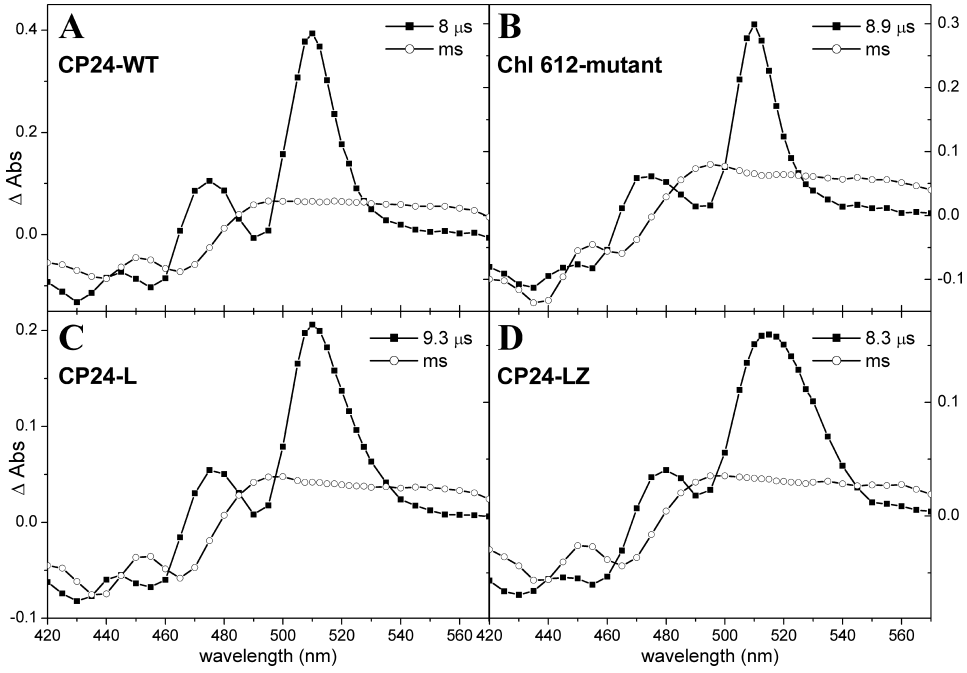

FIGURE 6. **TmS spectra of CP24 complexes in anaerobic conditions obtained by analysis of the decay kinetics.** The spectral components were determined by global fitting of the kinetics in the 200-ns to 5-ms range. *A*, CP24-WT; *B*, Chl 612-mutant; *C*, CP24-L; *D*, CP24-LZ. *Abs*, absorption.

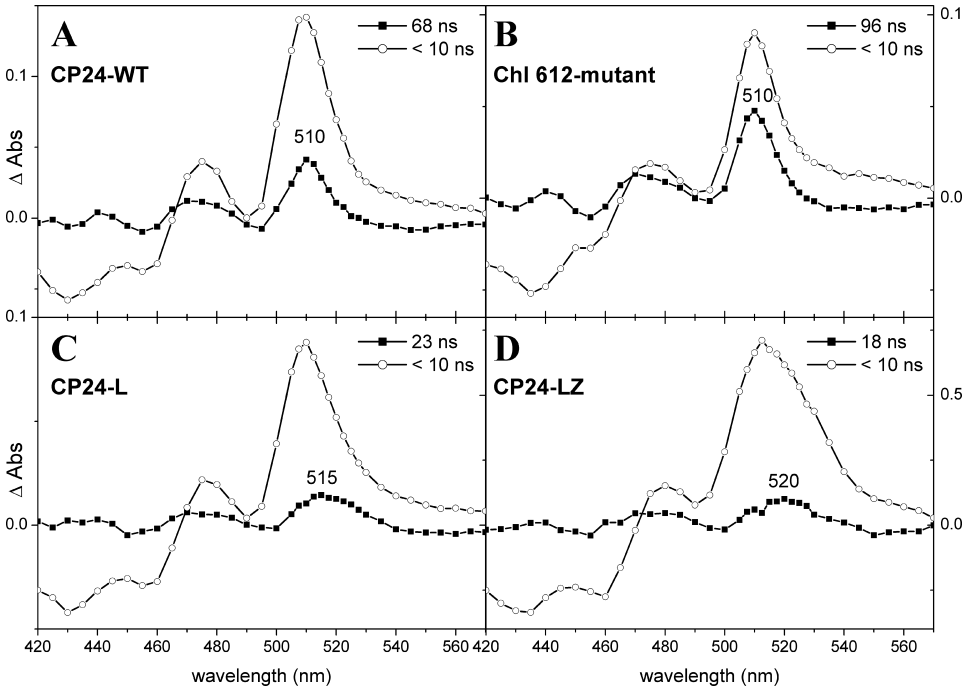

FIGURE 7. **TmS spectra of CP24 complexes in anaerobic conditions obtained by analysis of the rising kinetics.** The spectral components were determined by global fitting of the kinetics in the 7.5 ns to 200 ns range. Additional Chl triplet contributions are not shown. *A*, CP24-WT; *B*, Chl 612-mutant; *C*, CP24-L; *D*, CP24-LZ. *Abs*, absorption.

tion region around 500 nm, suggesting changes in xanthophyll-Chl *a* interactions.

Functional Measurements: Light Harvesting and Photoprotection

Carotenoids are involved in several photoprotective mechanisms: on one side they are able to quench Chl triplets, thus avoiding the formation of singlet oxygen (49); on the other side it has been proposed that they are involved in the quenching of Chl singlet excitations under high light conditions (6, 7). To test the role of the xanthophylls associated with CP24 in these two processes, time-resolved measurements were performed detecting changes in absorption, in the microsecond to millisecond range, and in fluorescence, in the picosecond to nanosecond range. To discriminate between the carotenoid binding sites, we have analyzed the mutants that are partially lacking lutein in L1 (Chls 612- and 610-mutants) and the complexes with different L2 occupancy (CP24-L, CP24-LZ) and made a comparison with the WT complex.

Triplet-minus-Singlet Measurements (TmS)—TmS measurements were performed at room temperature in the presence (see supplemental Fig. S2) and in the absence of oxygen (Figs. 6 and 7).

In anaerobiosis the decay kinetic of the WT could be fitted with two exponentials: a fast one with a lifetime of 8 μs, associated with the decay of the carotenoid triplets and a slow one in the millisecond range, corresponding to the spectrum of Chl triplets showing the contribution of both Chl *a* and Chl *b* (Fig. 6*A*). The maximum of the carotenoid triplet spectrum is at 510 nm, 3 nm red-shifted compared with the maxima obtained for both CP29 and CP26, indicating that the triplet transitions of the carotenoids in CP24 are at somewhat lower energy than in the other Lhcb monomeric complexes (50). The triplet transfer from Chls to carotenoids is around 70% (see *Experimental Procedures*), thus far lower than in the case of the other antenna complexes where it was 90–95% (50, 51), indicating the presence of a larger amount of unprotected Chls. This can partly be explained by the lower stability of CP24, which leads to the presence of a pool of unconnected Chls in the preparation. However, as judged from the fluorescence emission measurements (data not shown), the pool of Chls that do not participate to the energy transfer process is lower than 5% and can thus not fully account for the 30% of Chl triplets observed in the sample.

The decay kinetic of Chl 612-mutant is also described with two components: a carotenoid triplet decaying with a time constant of 8.9 μs and the Chl triplets decaying on millisecond time scale (Fig. 6*B*). The shape of the carotenoid component is very similar to that of the WT, despite the loss of half of the lutein in site L1 for the mutant. This suggests that the triplet spectra of violaxanthin-L2 and lutein-L1 are very similar. The triplet transfer efficiency drops below 50%, indicating that a higher number of Chls is unprotected in this complex. This was indeed expected considering that more than half of the ensemble is composed of complexes lacking lutein in the L1 site. In confirmation of this, the Chl triplet spectrum shows a higher contribution of Chls *a* (more intense bleaching at 430 nm) compared with the spectrum of the WT. Indeed, the lutein in the L1 site is located close to Chls *a*, which are not able to transfer triplets in the part of the ensemble that is lacking this xanthophyll.

Two components with lifetimes similar to those in WT can be observed in CP24-L and in CP24-LZ (Fig. 6, *C* and *D*). The spectra of the carotenoid triplet are broader and red-shifted (the maximum of CP24-LZ is at 515 nm) compared with the WT, signifying that all xanthophylls in the L2 site are active in photoprotection. The triplet transfer efficiency in CP24-LZ is identical to that of the WT, whereas it is slightly lower (around 60%) for CP24-L. This indicates that the substitution violaxanthin/zeaxanthin does not perturb the structure, at variance with LHCII, where it does lead to a significant perturbation (50).

To obtain information about the Chl-to-carotenoid triplet transfer, the rise kinetics of the TmS measurements were analyzed (Fig. 7). In all cases two components (plus an additional component representing the Chl triplets) were necessary to describe the kinetics satisfactorily. In all samples, the fast component has a lifetime shorter than 10 ns (because of the time resolution of the instrument, we cannot confidently assign a specific value to the lifetime in this time range). In the WT, the slow transfer occurs with a lifetime of around 70 ns. The spectra of the two components are very similar in the carotenoid triplet region, but in the Chl singlet region the spectrum associated with the fast component shows mainly bleaching at 430 nm, which is attributed to Chl *a*, whereas bleaching in both Chl *a* and Chl *b* region is observed in the spectrum of the slow component (Fig. 7*A*). The amplitude of the two components is also markedly different, with 80% of the carotenoid spectrum rising in less than 10 ns and only 20% in ~70 ns. The analysis of the Chl 612-mutant (Fig. 7*B*) gives similar results: two components with similar spectra were detected, but the intensity of the fast component was decreased compared with the WT. This suggests that the fast component is associated mainly with lutein-L1 and the slow component with violaxanthin-L2 and that lutein is in close contact with Chl *a* molecules, whereas both Chls *a* and Chls *b* are in close contact with violaxanthin in L2, in agreement with the results of the mutation analysis.

In the case of CP24-L and CP24-LZ, still two components are visible (Fig. 7, *C* and *D*), but the difference in lifetimes between them is small with the second component being as fast as ~20 ns. This gives some degree of uncertainty to both the spectra and the lifetimes. However, in both samples, the slow component is red-shifted compared with the slow component of the WT (to 515 nm in CP24-L and to 520 nm in CP24-LZ), suggesting that it is associated with lutein or zeaxanthin, which have substituted for violaxanthin in the L2 site, in agreement with the previous assignment.

TABLE 2
Chlorophyll fluorescence decay analysis of CP24 complexes
τ, lifetime; A, relative amplitude; $<\tau>$, amplitude average lifetime.

Sample	τ_1	A_1	τ_2	A_2	τ_3	A_3	$<\tau>$
	ns		*ns*		*ns*		*Ns*
CP24-WT	0.24	0.11	2.22	0.50	3.80[a]	0.40	2.65
CP24-L	0.29	0.10	1.42	0.41	3.10	0.50	2.14
CP24-LZ	0.33	0.11	1.44	0.53	2.81	0.36	1.81
Chl 610-mutant	0.16	0.20	1.73	0.32	3.81	0.48	2.43
Chl 612-mutant	0.20	0.16	1.95	0.47	3.64	0.37	2.29

[a] This value has been fixed because of the relatively short time window of the measurement which led to an unrealistic long component; however, the average lifetime did not change.

Time-resolved Fluorescence—The fluorescence kinetic decays of CP24-WT and mutants were measured upon excitation at 475 nm and detection at 680 nm. The choice of excitation/emission wavelengths was made to limit the effect of the presence of disconnected Chls: Chl *a* is not excited at 475 nm, and Chl *b* is hardly detected at 680 nm, so only the lifetimes of complexes in which a Chl *b* to Chl *a* transfer takes place are measured.

CP24-WT was fitted to a sum of three exponential decays, and it shows an average lifetime of 2.7 ns (Table 2). This value is half of the value of Chl *a* in solution (~6 ns), thus indicating that the complex is in a partially quenched state (50% of the fluorescence yield). This effect, although less strong, has been observed previously on other antenna complexes (52–55), and it has been suggested to be due to mixing of the excited state of Chls and carotenoids, which opens a dissipation channel via the short lived carotenoid S_1 state (45, 56).

To test this hypothesis, we have analyzed the Chl-mutants that lose lutein from the L1 site and the complexes reconstituted with lutein and lutein/zeaxanthin, where the substitution takes place in L2. The decay curves of all complexes were fitted to a sum of three exponential decays. Mutants for Chl 610 and 612 (Table 2) show a decrease in excited-state lifetime, respectively, of 6 and 11% compared with the WT, indicating that neither the Chls lost by mutation nor the lutein in the L1 site is responsible for the observed short lifetime of CP24 in solution. CP24-L and CP24-LZ have lifetimes that are, respectively, 20 and 33% shorter than that of the WT. This result clearly indicates that both lutein and zeaxanthin induce a certain degree of quenching in solution when located in the L2 site of CP24.

DISCUSSION

CP24 Versus the Other Members of the Lhcb Family

Structural Implications—The results of the mutation analysis indicate a slightly different folding of CP24 compared with the other Lhcb complexes (38–40): (i) mutations targeting residues in the helices B or C strongly affect the stability of CP24, as could be assessed by the low reconstitution yield of most of these mutants, whereas the same mutations were yielding relatively stable complexes for all other Lhcbs; (ii) in contrast to the other Lhcbs, the mutant lacking the ligand for Chl 610 yielded a stable reconstituted complex, whereas the one lacking the

ligand for Chl 603 could not. Both of these ligands are Glu and in LHCII they are also forming ionic bridges with Arg located in the opposite helix, contributing to the stability of the complex (57). The results indicate that in CP24 the ionic bridge between Glu^{62} and Arg^{193} is important for the stability and not the one formed by Glu^{188} and Arg^{67}, as is the case of the other Lhcbs. (iii) A stable CP24 complex with the L1 carotenoid binding site empty could be obtained (Chl 610- and 612-mutants), whereas the occupancy of this site was necessary for the stability of all other Lhcbs. It can be concluded that the stability of CP24 is determined by the helices B-C domain and not, as for the other Lhcs, by the one around the L1 carotenoid binding site.

Pigment Binding and Site Occupancy—Comparison of the pigment composition of CP24 with that of the other Lhcbs reconstituted under the same conditions (42) shows that CP24 is the complex with the lowest Chl *a*/*b* ratio. Our results reveal that this difference is due to two effects: (i) the absence of Chl 613 and 614 binding sites, which in LHCII and in the other antenna complexes have a preferential affinity for Chls *a*; (ii) the presence of Gln as a ligand for Chl 606, which leads to a high Chl *b* occupancy in the helix C domain. In LHCII, this residue forms H-bonds with the formyl groups of Chls *b* 607 and 609, thus favoring the binding of Chl *b* in these two sites (12), whereas in the Lhc antennas in which this Gln is substituted by Glu, site 609 can be occupied by both Chl *a* and Chl *b* (38, 39). In agreement, our results show that in CP24, like in LHCII, sites 609 and 606 are occupied by Chl *b*.

Considering that Chls 601 and 605 are not present even in recombinant LHCII, it can be concluded that the 10 Chls coordinated to recombinant CP24 correspond to sites 602–604 and 606–612 in LHCII, with Chls *a* accommodated at sites 610, 611, 612, and likely 602 and 603, and Chls *b* at all other sites. CP24-WT also binds lutein in the L1 site and violaxanthin in the L2 site, with lutein-L1 absorbing at 496 nm and violaxanthin-L2 at 499 nm. It can be noted that in CP24 the L2 site induces a larger red shift of the xanthophyll absorption than in the other monomeric Lhcb complexes (30, 31, 58).

The data indicate that the absorption bands at 680 and 670 nm are associated with Chls 610, 611, and 612, with the strongly interacting 611/612 pair representing the lowest energy state of the system. According to the fitting (Fig. 1), two more Chls *a* absorb around 675 nm, and, although we could not obtain a clear answer from the analysis of the mutants, they are tentatively associated with Chls 602 and 603, which absorb at these wavelengths in LHCII (39).

A summary of the results is presented in Fig. 8 integrated in a structural model of CP24 obtained using the sequence of CP24 and the structure of LHCII as template. The model also shows a long stromal loop, which is peculiar for CP24 and can be involved in interactions with other subunits.

Role of Individual Pigments in Light Harvesting and Photoprotection

The average excited-state lifetime of CP24 WT is 2.7 ns, whereas it is ~6 ns for Chls *a* in solution. A shorter lifetime than Chl in solution was observed also for other antenna complexes (52–55), indicating that the Chls in protein environment are partially quenched. It was proposed that strong interactions

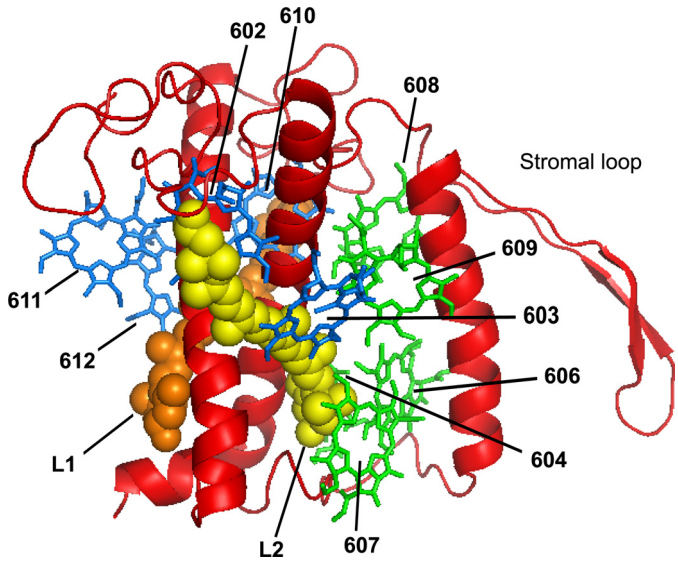

FIGURE 8. **Structural model of CP24.** The model was obtained in SwissModel Workspace using the sequence of CP24 and the structure of LHCII (PDB code 1rwt) as template. The position of the Chls is that of LHCII (as well as the nomenclature), but only the Chls present in CP24 (this work) are shown. Chl *a*, *blue*; Chl *b*, *green*; lutein in L1, *orange*; violaxanthin in L2, *yellow*. The long stromal loop is not present in the template and cannot be modeled correctly.

between Chls and carotenoids, which can act as a fast decay channel, are responsible for the observed quenching (45, 56). Analysis of the CP24 mutants allows us to check for the involvement in this process of the xanthophylls in sites L1 and L2. The absence of lutein in L1 does not change the amount of quenching; therefore, this xanthophyll is not responsible for the quenching of CP24 in solution. In contrast, the shorter lifetime, compared with that of the WT, of mutants of Chl 610 and 612, which in addition to lutein also lose Chls, is in agreement with the presence of a quenching site located in a different domain of the complex. Indeed, Boltzmann distribution calculations in CP24-WT, using the spectral forms and the site energies obtained from the fitting in Fig. 2, indicate that at equilibrium 60% of the energy is located in the domain formed by Chls 610/611/612. The removal of these Chls (as in the mutants) changes the Boltzmann energy distribution in the complex, increasing the probability of populating the quencher and thus leading to a shortening of the lifetime.

In addition, the data show that the lifetime of the complex can be modulated by the occupancy of site L2 by different xanthophylls, thus suggesting a central role for this site in the quenching in solution. In principle, in the L2 site the xanthophyll can act in two ways: (i) as direct quencher, via a strong interaction with a neighboring Chl or (ii) indirectly, inducing a conformational change in the complex which creates a quencher located in a different protein domain. The TmS measurements represent a tool to discriminate between these two possibilities. The triplet transfer is very sensitive to even small changes in the organization of the pigments because the transfer rate depends exponentially on the distance between donor and acceptor (59). In the WT complex, two Chl to carotenoid triplet transfer components were detected: a fast transfer (less than 10 ns) toward lutein-L1 and a slow one (around 70 ns) toward violaxanthin-L2. Upon substitution of violaxanthin

with lutein or zeaxanthin, the second transfer component becomes faster (around 20 ns). The triplet spectrum of the Chls is broad and flat, and the three xanthophylls have similar energy when bound to the L2 site of CP24 (see above), suggesting that the overlap integral between Chls and violaxanthin, lutein, or zeaxanthin is very similar. The increase in transfer rate, in the presence of zeaxanthin and lutein, is thus mainly due to a decrease in the distance between Chls and carotenoid L2. This also implies that lutein or zeaxanthin in the L2 site interacts stronger with neighboring Chls than violaxanthin, thus possibly creating a dissipative channel. This can occur via a strong excitonic interaction between the two chromophores (45) or via the formation of a carotenoid radical cation (7). Although the presence of a zeaxanthin radical cation has been detected in CP24 in solution, it occurs only in 1% of the population (7), and it thus cannot explain the observed decrease of 30% of the excited-state lifetime. It should be concluded that in solution, the major quenching mechanism involves a strong interaction between zeaxanthin or lutein and a neighboring Chl, which creates a fast dissipation channel likely via the short living S1 state of the xanthophylls. This implies that one of the Chls located in close proximity to the xanthophyll in L2 is involved in the quenching. Unfortunately, none of the mutants targeting Chls close to the L2 site was stable enough to allow fluorescence time-resolved measurements. However, in CP26 the absence of Chl 603 induces a large increase of the fluorescence yield of the complex (40). Considering that Chl 603 is located in close contact with the carotenoid in L2, it is likely that it is responsible for the quenching also in CP24. In addition, in CP29, the absence of Chl 603 abolishes the formation of the zeaxanthin radical cation (7). Taken together, the data suggest that, in the minor antenna complexes, a strong interaction between Chl 603 and the carotenoid in L2 is present when this site is occupied by lutein or zeaxanthin, which can also lead to the formation of a radical cation, although the latter does not represent the mainstream of the decay in solution. Although the amount of quenching observed in solution is not sufficient to explain NPQ *in vivo* fully (60), it is possible that *in vivo*, where other factors (*e.g.* PsbS, ΔpH, protein-protein interactions) come into play (53, 61), the observed effect caused by the presence of zeaxanthin in the L2 site is enhanced, leading to a stronger quenching, as suggested previously (23).

In vivo fluorescence induction measurements showed that the *Arabidopsis* double mutant lacking CP24 and CP26 has a NPQ rise kinetic slower than the WT (21). This was attributed to the absence of zeaxanthin-binding proteins, thus suggesting that CP24 is involved in the zeaxanthin-dependent quenching. TmS data support the idea that the binding of zeaxanthin to the L2 site of CP24 is functional. Different from LHCII, in which the binding of zeaxanthin in the internal sites leads to a destabilization of the complex (30) and to a strong decrease of the triplet quenching efficiency (50), in CP24 the presence of zeaxanthin in the L2 site does not destabilize the complex and ensure a triplet quenching identical to the WT. This supports the idea of a different role of CP24 and LHCII *in vivo*, where CP24, but not LHCII, is expected to be able to exchange violaxanthin for zeaxanthin in the L2 site during the activity of the xanthophyll cycle (62), thus participating to the zeaxanthin-dependent quenching (63).

CONCLUSIONS

Previous *in vivo* and *in vitro* work has suggested that CP24 is involved in the NPQ process, and it contains one of the possible quenching sites. In this work we have searched for the quenching site integrating mutation analysis with time-resolved spectroscopy. The occupancy of the individual binding sites and the spectroscopic properties of each chromophore in each binding site were revealed. The lowest energy state of the complex is constituted by Chls 611/612, and it is not responsible for the low fluorescence yield of the complex in solution. Also, lutein in the L1 site is not involved in the quenching in solution. The data indicate that in CP24 the occupancy of the L2 carotenoid binding site modulates the function of the protein, allowing the conversion of the complex from a light-harvesting to a dissipative state. In normal conditions, CP24 binds violaxanthin in the L2 site, but this xanthophyll can be exchanged for zeaxanthin in stress conditions. Zeaxanthin in this site is located closer to Chls than violaxanthin, suggesting that it might be involved in a strong interaction with a Chl, creating a dissipative channel. This mechanism, which we have observed *in vitro*, is in agreement with very recent results obtained upon *in vivo* measurements, which suggest that the quenching is due to a Chl-zeaxanthin interaction (64).

Acknowledgments—We thank Arie van Hoek from the Micro-Spectroscopy Center of Wageningen University for excellent technical support and Stefano Caffarri for sequence alignment in Fig. 1.

REFERENCES

1. Jansson, S. (1999) *Trends Plant Sci.* **4,** 236–240
2. Barber, J., and Andersson, B. (1992) *Trends Biochem. Sci.* **17,** 61–66
3. DemmigAdams, B., and Adams, W. W. (1992) *Annu. Rev. Plant Physiol. Plant Mol. Biol.* **43,** 599–626
4. Horton, P., and Ruban, A. (2005) *J. Exp. Bot.* **56,** 365–373
5. Briantais, J. M. (1994) *Photosynth. Res.* **40,** 287–294
6. Ruban, A. V., Berera, R., Ilioaia, C., van Stokkum, I. H. M., Kennis, J. T. M., Pascal, A. A., van Amerongen, H., Robert, B., Horton, P., and van Grondelle, R. (2007) *Nature* **450,** 575–578
7. Ahn, T. K., Avenson, T. J., Ballottari, M., Cheng, Y. C., Niyogi, K. K., Bassi, R., and Fleming, G. R. (2008) *Science* **320,** 794–797
8. Miloslavina, Y., Wehner, A., Lambrev, P. H., Wientjes, E., Reus, M., Garab, G., Croce, R., and Holzwarth, A. R. (2008) *FEBS Lett.* **582,** 3625–3631
9. Caffarri, S., Croce, R., Cattivelli, L., and Bassi, R. (2004) *Biochemistry* **43,** 9467–9476
10. Dekker, J. P., and Boekema, E. J. (2005) *Biochim. Biophys. Acta* **1706,** 12–39
11. Boekema, E. J., Hankamer, B., Bald, D., Kruip, J., Nield, J., Boonstra, A. F., Barber, J., and Rögner, M. (1995) *Proc. Natl. Acad. Sci. U.S.A.* **92,** 175–179
12. Liu, Z., Yan, H., Wang, K., Kuang, T., Zhang, J., Gui, L., An, X., and Chang, W. (2004) *Nature* **428,** 287–292
13. Standfuss, R., van Scheltinga, A. C. T., Lamborghini, M., and Kühlbrandt, W. (2005) *EMBO J.* **24,** 919–928
14. Dainese, P., and Bassi, R. (1991) *J. Biol. Chem.* **266,** 8136–8142
15. Koziol, A. G., Borza, T., Ishida, K., Keeling, P., Lee, R. W., and Durnford, D. G. (2007) *Plant Physiol.* **143,** 1802–1816
16. Peter, G. F., and Thornber, J. P. (1991) *J. Biol. Chem.* **266,** 16745–16754
17. Ruban, A. V., Young, A. J., Pascal, A. A., and Horton, P. (1994) *Plant Physiol.* **104,** 227–234

18. Pagano, A., Cinque, G., and Bassi, R. (1998) *J. Biol. Chem.* **273,** 17154–17165
19. Wehner, A., Grasses, T., and Jahns, P. (2006) *J. Biol. Chem.* **281,** 21924–21933
20. Kovács, L., Damkjaer, J., Kereïche, S., Ilioaia, C., Ruban, A. V., Boekema, E. J., Jansson, S., and Horton, P. (2006) *Plant Cell* **18,** 3106–3120
21. de Bianchi, S., Dall'Osto, L., Tognon, G., Morosinotto, T., and Bassi, R. (2008) *Plant Cell* **20,** 1012–1028
22. Holt, N. E., Zigmantas, D., Valkunas, L., Li, X. P., Niyogi, K. K., and Fleming, G. R. (2005) *Science* **307,** 433–436
23. Avenson, T. J., Ahn, T. K., Zigmantas, D., Niyogi, K. K., Li, Z., Ballottari, M., Bassi, R., and Fleming, G. R. (2008) *J. Biol. Chem.* **283,** 3550–3558
24. Betterle, N., Ballottari, M., Zorzan, S., de Bianchi, S., Cazzaniga, S., Dall'Osto, L., Morosinotto, T., and Bassi, R. (2009) *J. Biol. Chem.* **284,** 15255–15266
25. Li, X. P., Björkman, O., Shih, C., Grossman, A. R., Rosenquist, M., Jansson, S., and Niyogi, K. K. (2000) *Nature* **403,** 391–395
26. Teramoto, H., Ono, T., and Minagawa, J. (2001) *Plant Cell Physiol.* **42,** 849–856
27. Elrad, D., Niyogi, K. K., and Grossman, A. R. (2002) *Plant Cell* **14,** 1801–1816
28. Finazzi, G., Johnson, G. N., Dall'Osto, L., Zito, F., Bonente, G., Bassi, R., and Wollman, F. A. (2006) *Biochemistry* **45,** 1490–1498
29. Bonente, G., Passarini, F., Cazzaniga, S., Mancone, C., Buia, M. C., Tripodi, M., Bassi, R., and Caffarri, S. (2008) *Photochem. Photobiol.* **84,** 1359–1370
30. Croce, R., Weiss, S., and Bassi, R. (1999) *J. Biol. Chem.* **274,** 29613–29623
31. Croce, R., Canino, G., Ros, F., and Bassi, R. (2002) *Biochemistry* **41,** 7334–7343
32. Gilmore, A. M., and Yamamoto, H. Y. (1991) *Plant Physiol.* **96,** 635–643
33. Croce, R., Mozzo, M., Morosinotto, T., Romeo, A., Hienerwadel, R., and Bassi, R. (2007) *Biochemistry* **46,** 3846–3855
34. Somsen, O. J., Keukens, L. B., de Keijzer, M. N., van Hoek, A., and van Amerongen, H. (2005) *Chemphyschem* **6,** 1622–1627
35. van Oort, B., Amunts, A., Borst, J. W., van Hoek, A., Nelson, N., van Amerongen, H., and Croce, R. (2008) *Biophys. J.* **95,** 5851–5861
36. Digris, A. V., Skakoun, V. V., Novikov, E. G., van Hoek, A., Claiborne, A., and Visser, A. J. (1999) *Eur. Biophys. J.* **28,** 526–531
37. Arnold, K., Bordoli, L., Kopp, J., and Schwede, T. (2006) *Bioinformatics* **22,** 195–201
38. Bassi, R., Croce, R., Cugini, D., and Sandonà, D. (1999) *Proc. Natl. Acad. Sci. U.S.A.* **96,** 10056–10061
39. Remelli, R., Varotto, C., Sandonà, D., Croce, R., and Bassi, R. (1999) *J. Biol. Chem.* **274,** 33510–33521
40. Ballottari, M., Mozzo, M., Croce, R., Morosinotto, T., and Bassi, R. (2009) *J. Biol. Chem.* **284,** 8103–8113
41. Plumley, F. G., and Schmidt, G. W. (1987) *Proc. Natl. Acad. Sci. U.S.A.* **84,** 146–150
42. Caffarri, S., Passarini, F., Bassi, R., and Croce, R. (2007) *FEBS Lett.* **581,** 4704–4710
43. Cinque, G., Croce, R., and Bassi, R. (2000) *Photosynth. Res.* **64,** 233–242
44. Mozzo, M., Passarini, F., Bassi, R., van Amerongen, H., and Croce, R. (2008) *Biochim. Biophys. Acta* **1777,** 1263–1267
45. van Amerongen, H., and van Grondelle, R. (2001) *J. Phys. Chem. B* **105,** 604–617
46. Morosinotto, T., Baronio, R., and Bassi, R. (2002) *J. Biol. Chem.* **277,** 36913–36920
47. Young, A., and Britton, G. (eds) (1993) *Carotenoids in Photosynthesis*, Chapman and Hall, Suffolk
48. Mozzo, M., Morosinotto, T., Bassi, R., and Croce, R. (2006) *Biochim. Biophys. Acta* **1757,** 1607–1613
49. SiefermannHarms, D. (1987) *Physiol. Plant.* **69,** 561–568
50. Mozzo, M., Dall'Osto, L., Hienerwadel, R., Bassi, R., and Croce, R. (2008) *J. Biol. Chem.* **283,** 6184–6192
51. Barzda, V., Peterman, E. J., van Grondelle, R., and van Amerongen, H. (1998) *Biochemistry* **37,** 546–551
52. Crimi, M., Dorra, D., Bösinger, C. S., Giuffra, E., Holzwarth, A. R., and Bassi, R. (2001) *Eur. J. Biochem.* **268,** 260–267
53. Moya, I., Silvestri, M., Vallon, O., Cinque, G., and Bassi, R. (2001) *Biochemistry* **40,** 12552–12561
54. Palacios, M. A., de Weerd, F. L., Ihalainen, J. A., van Grondelle, R., and van Amerongen, H. (2002) *J. Phys. Chem. B* **106,** 5782–5787
55. Ihalainen, J. A., Croce, R., Morosinotto, T., van Stokkum, I. H., Bassi, R., Dekker, J. P., and van Grondelle, R. (2005) *J. Phys. Chem. B* **109,** 21150–21158
56. Lampoura, S. S., Barzda, V., Owen, G. M., Hoff, A. J., and van Amerongen, H. (2002) *Biochemistry* **41,** 9139–9144
57. Kühlbrandt, W., Wang, D. N., and Fujiyoshi, Y. (1994) *Nature* **367,** 614–621
58. Frank, H. A., Das, S. K., Bautista, J. A., Bruce, D., Vasil'ev, S., Crimi, M., Croce, R., and Bassi, R. (2001) *Biochemistry* **40,** 1220–1225
59. Dexter, D. L. (1953) *J. Chem. Phys.* **21,** 836–850
60. DemmigAdams, B., Adams, W. W., Barker, D. H., Logan, B. A., Bowling, D. R., and Verhoeven, A. S. (1996) *Physiol. Plant.* **98,** 253–264
61. Bassi, R., and Caffarri, S. (2000) *Photosynth. Res.* **64,** 243–256
62. Demmig-Adams, B., Adams, W. W., Heber, U., Neimanis, S., Winter, K., Krüger, A., Czygan, F. C., Bilger, W., and Björkman, O. (1990) *Plant Physiol.* **92,** 293–301
63. Johnson, M. P., Pérez-Bueno, M. L., Zia, A., Horton, P., and Ruban, A. V. (2009) *Plant Physiol.* **149,** 1061–1075
64. Bode, S., Quentmeier, C. C., Liao, P. N., Hafi, N., Barros, T., Wilk, L., Bittner, F., and Walla, P. J. (2009) *Proc. Natl. Acad. Sci. U.S.A.* 106, 12311–12316